Regular Article

PHYSICAL CHEMISTRY RESEARCH
Published by the
Iranian Chemical Society
www.physchemres.org
info@physchemres.org

***Phys. Chem. Res.**, Vol. 7, No. 3, 681-699, September 2019*
DOI: 10.22036/pcr.2019.176484.1606

Spectroscopic, Docking and Molecular Dynamics Simulation Studies on the Interaction of Etofylline and Human Serum Albumin

D. Mohammad-Aghaie*, F. Hamedi and M.N. Soltani Rad

Department of Chemistry, Shiraz University of Technology, Shiraz 71555-313, Iran

(Received 20 March 2019, Accepted 18 August 2019)

The purpose of this study is to investigate the interaction of etofylline, as an established drug for asthma remedy, with the major transport protein in human blood circulation, the human serum albumin (HSA). In this respect, the fluorescence and circular dichroism (CD) spectroscopy techniques, along with the molecular docking and molecular dynamics simulation methods were employed. Analysis of the fluorescence quenching data with the Stern-Volmer equation confirmed the static quenching mechanism due to the etofylline-HSA complex formation. Calculated thermodynamics parameters ($\Delta H < 0$ and $\Delta S > 0$) indicated that the binding mechanism is both enthalpy and entropy driven, while simultaneous hydrophobic and hydrogen bonding interactions are involved in the etofylline-HSA interaction. The CD spectrum demonstrated some conformational alterations of HSA upon etofylline addition. Moreover, the distance between tryptophan residue of HSA and etofylline was calculated by the Forster's non-radiative energy transfer theory (FRET). The result was in good accordance with the molecular docking outcome.

Keywords: Etofylline, Human serum albumin, Spectroscopy, Molecular modeling

INTRODUCTION

Among several transport proteins in blood, HSA is the most abundant protein, which is synthesized and secreted from liver cells [1-3]. Serum albumin is a soluble, monomeric protein, necessary for maintaining and regulating the colloidal osmotic pressure of blood [4-6]. It is used to increase the circulating osmotic plasma volume, thereby reducing hemoconcentration and blood viscosity. Albumin serves also as a transport protein, carrying large organic anions, including fatty acids, bilirubin, many drugs, and also hormones, such as cortisol and thyroxine. Its capability in binding to drugs and other endogenous and exogenous molecules results in selective delivery of such compounds [7-9].

According to X-ray crystallographic analyses of human serum albumin and its recombinant version, the polypeptide chain forms a heart-shaped protein, consisting of 585 amino acid residues [3]. HSA has a molecular mass of 66.5 kDa [10], and is composed of 67% α-helix, but no β-sheet, and can be divided into three homologous domains (I-III), while each of them is comprised of two subdomains (A and B) [11]. Binding of drugs to human serum albumin is an area of intense research [12], since the pharmacokinetics and pharmacodynamics of drugs are strongly affected by their binding to this protein [1,8]. These interactions which influence distribution, bioavailability and elimination of ligands [6,9,13] can even alter solubility of drugs and reduce their toxicity [14].

Investigating the drug binding to HSA, along with identifying the drug binding site on HSA molecule, are important for pharmacokinetics. It is known that drug binding to plasma proteins, varies from near zero to over 99%, depending upon the drug's nature. The remaining unbound drug is available to pass through the cell membranes and exert its effect. Drug binding to HSA increases its half-life and lowers the free drug concentration in blood making it extremely important for clinical care. In

*Corresponding author. E-mail: d_aghaie@sutech.ac.ir

early stage of drug discovery, its binding to plasma protein is important to determine, because it is used to evaluate the needs for drug dosing and clearance from body. In this regard, design of new and more effective drugs along with perceiving their pharmacokinetic properties, requires a knowledge of drug-protein (especially drug-HSA) interactions [15].

This study aims to assess the interactions of HSA with etofylline. Among the asthma bronchodilators, theophylline has kept its important role as a potent and useful drug. Etofylline (the ethyl salt of theophylline) is also a bronchodilator and normally is applied in combination with theophylline. Unlike other xanthine derivatives, etofylline is stable and does not metabolize into theophylline in the body [16]. On the other hand, due to the low solubility of theophylline in water, it cannot be administered by infusion, hence some water soluble theophylline derivatives, such as etofylline are applied when injection is required [17]. It is noteworthy that combination of etofylline and theophylline exhibits less frequent adverse side effects than an equivalent dose of theophylline alone. Chemically known as 7-(2-hydroxyethyl)-1,3-dimethylpurine-2,6-dione, the structure of etofylline is shown in Fig. 1 [16].

Considering the reasons mentioned, knowledge on the interaction of etofylline with HSA, can help to unravel the metabolic profile of this drug. To the best of our knowledge, this interaction has not been yet studied, thus in this research the fluorescence and CD spectroscopies were applied to investigate the interaction of etofylline with HSA. Later, in order to identify the binding mechanism and binding parameters, the Stern-Volmer and Van′t Hoff equations were utilized.

In addition, molecular dynamics (MD) and docking simulations at different temperatures were performed to specify the thermodynamic parameters and the binding sites. Finally, MD simulation on the etofylline-HSA complex could shed light on the protein-drug interaction from microscopic point of view.

MATERIALS AND METHODS

Materials

HSA was purchased from Sigma chemical company and used without further purification, while etofylline was synthesized by the known method [18]. Concentration of

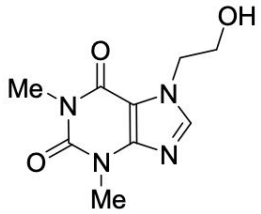

Fig. 1. Chemical structure of Etofylline.

HSA was determined by spectrophotometric method at λ = 280 nm and molar extinction coefficient of $\varepsilon = 35700\ M^{-1}\ cm^{-1}$ [19]. The solutions of HSA (10 μM) and etofylline (1 mM) were prepared by dissolving known amounts of the solid substances in 50 mM sodium phosphate buffer of pH 7.4. The solutions were used freshly after preparation and kept at 0-4 °C in the dark environment for maximum of 3 days, in order to make sure about the fixed pH value and maintaining the ionic strength of the solutions.

Methods

Fluorescence spectroscopy. HSA fluorescence measurements were carried out by a Cary-Eclipse fluorescence spectrophotometer (Varian Company, Australia) using a 1.0 cm optical path quartz cell and a circulating water bath. The excitation wavelength was 280 nm, and slits widths for excitation and emission were set at 5 nm. HSA solution (10 μM) was titrated by gradual additions of etofylline solution (1 mM), through microinjection (to give a concentration ranging from 0-75 μM). Fluorescence intensities were measured at three different temperatures (298, 303 and 310 K). All samples were kept for 3 min at a fixed temperature, then the emission spectra were recorded in the range of 285-500 nm. Control measurements were performed by addition of identical amounts of etofylline in the absence of HSA, therefore, the final spectra were acquired by subtracting the spectra of Etofylline in the absence of HSA, from the total spectra in its presence. All measurements were repeated for three times.

Synchronous fluorescence spectroscopy. Synchronous fluorescence spectroscopy (SFS) plays an important role in the simultaneous analysis of multicomponent samples, due to the remarkable advantages of spectral simplification, light scattering reduction, and selectivity improvement, over

conventional fluorescence spectroscopy [6,20]. On the other hand, SFS is a simple and effective method for measuring fluorescence quenching and the possible shift of the maximum emission wavelength (λ_{max}). It also can reflect the change of microenvironment around the chromophore. In this context, the $\Delta\lambda$ value (Scanning interval: $\Delta\lambda = \lambda_{emission} - \lambda_{excitation}$) of the specific fluorophore is employed as the principle scanning parameter. In addition, synchronous fluorescence spectra of HSA in the presence of different concentrations of ligand were recorded. $\Delta\lambda$ values of 15 and 60 nm were selected in synchronous fluorescence measurement of HSA, in order to extract the characteristic information of Tyr and Trp residues, respectively [21-24].

Circular dichroism spectroscopy. Circular dichroism is the difference in the absorption of left-handed and right-handed circulary polarized lights [(L-CPL) & (R-CPL)] and occurs when a molecule contains one or more chiral chromophores (light-absorbing groups). CD spectroscopy is a technique where the CD of molecules is measured over a range of wavelengths. Its primary use is in analyzing the secondary structure or conformation of macromolecules, particularly protein. Since the secondary structure is sensitive to its environment, temperature or pH, CD can be used to observe that how secondary structure changes with the environmental conditions or due to the interaction with other molecules. The CD spectra of HSA in the absence and presence of etofylline were recorded on a spectropolarimeter (Aviv, model 215, USA), using 0.1 cm path length cuvette, under a nitrogen atmosphere at 298 K. The HSA concentration was maintained constant at 10.0 μM, while 20, 40, 60 and 80 μl of etofylline with concentration of 1.0 mM were added to 250 μl of HSA. All spectra were recorded from 260 nm to 190 nm with a step size and bandwidth of 1 nm. 3 scans were accumulated and averaged for each system at an average time of 0.3 s.

Molecular dynamics simulation. The initial coordinates of HSA were obtained from the protein data bank (HSA: PDB entry code: 3tdl). This crystal structure consists of one HSA chain in complex with 11-(Dansylamino) undecanoic acid (DAUDA). The MDS was only carried out on the HSA chain, using the GROMACS 5.4.1 software package [25]. The topology and interaction parameters of HSA were created using the standard GROMOS96 43a1 force field [26], in which the nonbonded intermolecular potential is defined as a sum of the Lennard-Jones force and pairwise Coulombic interaction. Initial velocities were assigned to the atoms according to the Maxwell-Boltzmann [27] distribution, corresponding to 310 K, the simulation temperature.

After an insertion of HSA into a cubic box, with the side length of 10.6 nm^3, the box was filled by 36219 water molecules, (simple point charge, SPC water model [28]) to mimic the physiological conditions. Thirteen Na^+ counter ions were added by replacing water molecules to ensure overall charge neutrality of the simulated system. In order to optimize the position of water molecules and equilibrate the temperature and pressure of the system, the following steps were performed, successively.

(*i*) At first, the energy minimization was carried out using the steepest descent method [29] to release the conflicting contacts. (*ii*) The equilibration stage was conducted in two phases. The first phase was performed under an NVT ensemble, for 100 ps. This time was enough for the temperature of the system to reach a plateau, at the desired value. In the second phase, the equilibration of the pressure was conducted under an NPT ensemble, again for 100 ps. In both NVT and NPT equilibration phases, the protein was position-restrained to avoid drastic rearrangement of this critical part of the system, during the equilibration of the added solvent and counter ions.

(*iii*) After completion of these two equilibration phases, the position restraints were released and the full system was subjected to 20 ns of MDS.

The production run was also conducted under NPT ensemble, employing the Parrinello-Rahman barostat [30] and Berendsen thermostat [31] with coupled pressure and temperature at 1.0 bar and 310 K, respectively. Cut off distances for the calculation of electrostatic and van der Waals interactions were both set to 1.4 nm, while the Particle Mesh Ewald (PME) method [32-33] was used to treat the long-range electrostatic interactions.

The periodic boundary conditions were applied in 3 dimensions and the equations of motion were integrated by the leap-frog algorithm, with a time step of 2 fs. Linear constraint solver (LINCS) algorithm [34] was employed to fix the chemical bonds within the protein molecule, while the SETTLE algorithm [35] did the same mission for solvent molecules. The atom coordinates were recorded

every 1 ps during the MDS for later analysis.

In addition to the molecular dynamics simulation of HSA protein (with the aim to access its equilibrated structure, under physiological conditions), the docked HSA-etofylline complex was also simulated later, under the same method and conditions (described above) at 310 K. The required coordinates and topology parameters of etofylline were obtained from the PRODRG web server [36].

Molecular docking. The computational procedure of molecular docking aims to predict the favored orientation of etofylline drug to its target protein, HSA, when these are bound to each other to form a stable complex. As described in previous section, the crystal structure of HSA, taken from protein data bank was simulated and equilibrated at 310 K.

On the other hand, the chemical 3D-structure of etofylline was generated by the GaussView software, while the quantum chemistry program, Gaussian 09 [37] was later used for its energy minimization at the 3-21 G^* level, using the Hartree-Fock method. We employed AutoDock Vina [38] in order to dock etofylline to the HSA structure. This software uses a sophisticated gradient optimization method in its local optimization procedure.

Before docking, water molecules were removed from the protein's pdb file and the polar hydrogen atoms (required for appropriate treatment of electrostatic during docking) were added to both HSA and etofylline structures. Partial atomic Gasteiger charges [39] were also computed and assigned to every atoms of both ligand (etofylline) and receptor (HSA). The grid box of 114 × 108 × 126 dimensions, with 1.0 Å resolution was extended over all domains of HSA. During the docking process, the receptor taken from MD simulation was set rigid since it was in its most stable state, while the ligand was considered as a flexible molecule. Finally the PyMol version 1.8.6.0 and LigPlot$^+$ version v.1.4.5 programs were utilized to visualize and analyze the lowest energy docked conformation.

RESULTS AND DISCUSSION

Fluorescence Measurement

Fluorescence spectroscopy is an efficient method to investigate the interaction of various ligands with proteins [40-41]. Three aromatic amino acids, tyrosine, phenylalanine and tryptophan are responsible for intrinsic fluorescence of proteins. However, the main contribution of HSA intrinsic fluorescence is related to Trp 214 residue [42]. Excitation of Trp 214 in subdomain IIA of HSA at 280 nm gives rise to the characteristic emission spectra of this residue. The corresponding method is known as the conventional fluorescence spectroscopy. Note that the same spectra were taken from HSA, in the presence of different drug concentrations, in order to examine the conformational changes of this protein, due to possible protein-drug interactions. Figure 2 demonstrates that the fluorescence intensity of HSA is reduced owing to the HSA-etofylline interaction. Obviously, more added etofylline gives rise to the more decreased fluorescence intensity.

It is noteworthy to mention that although etofylline diminishes the fluorescence intensity of HSA, however, it cannot affect the position of maximum emission wavelength. This confirms that the surrounding polarity of Trp residue remains almost intact throughout the titration experiment.

Fluorescence Quenching Mechanism

Quenching refers to any process decreasing the fluorescence intensity of a given substance. A variety of processes can result in quenching, such as excited state reactions, energy transfer, complex formation and collisional quenching. The last two processes, known as the main quenching mechanisms, are called static and dynamic quenching, respectively, and are well distinguishable based on their different temperature dependence. For dynamic quenching, the quenching constant increases with the rising temperature, while an inverse correlation is valid for the static quenching. In this study, the well-known Stern-Volmer equation was employed to determine the quenching mechanism [43]:

$$\frac{F_0}{F} = 1 + K_{SV}[Q] = 1 + K_q \,.\, K_q \,.\, \tau_0[Q] \qquad (1)$$

In the above equation F_0 and F are respectively the fluorescence intensities in the absence and presence of a quencher, with concentration [Q]. K_{SV} is the Stern-Volmer quenching constant, k_q, the quenching rate constant, and τ_0, the average fluorescence lifetime of HSA in the absence of quencher, which is typically on the order of 10^{-8} s [44]. Figure 3 illustrates the F_0/F plots for HSA against [Q] at different temperatures and λ_{ex} = 280 nm.

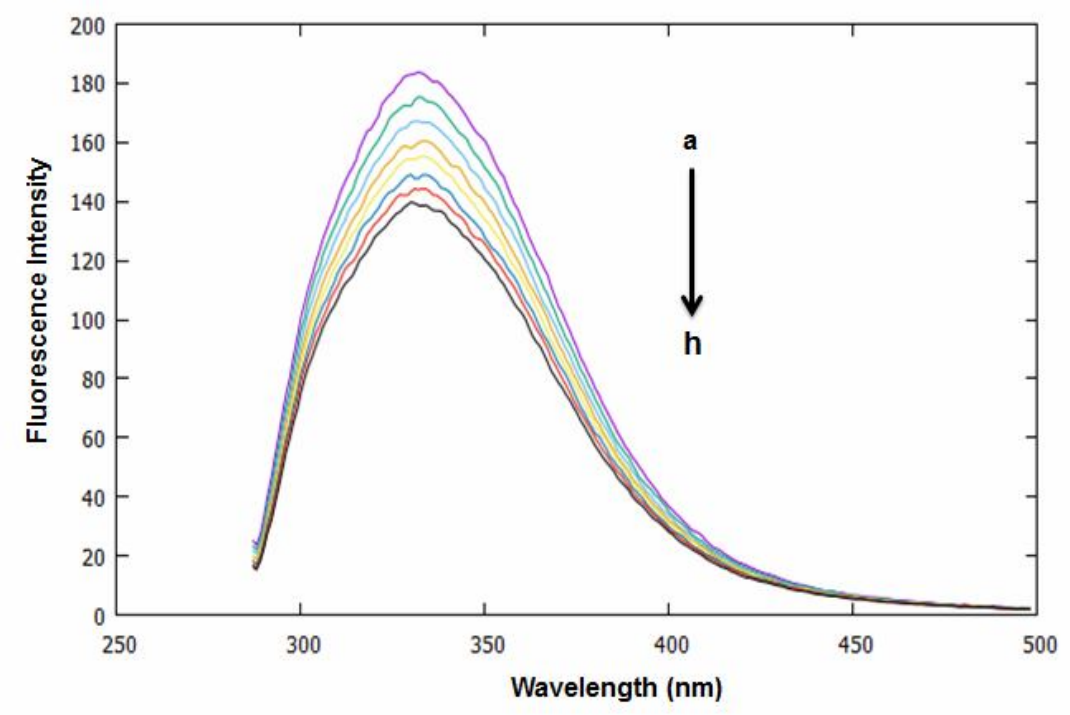

Fig. 2. The effect of adding different amounts of Etofylline stock solution (1 mM), on the fluorescence intensity of HSA (10 µM), at λ_{ex} = 280 nm. [(a-h) corresponds to 0, 10, 20, 30, 40, 50, 60 and 70 µl Etofylline].

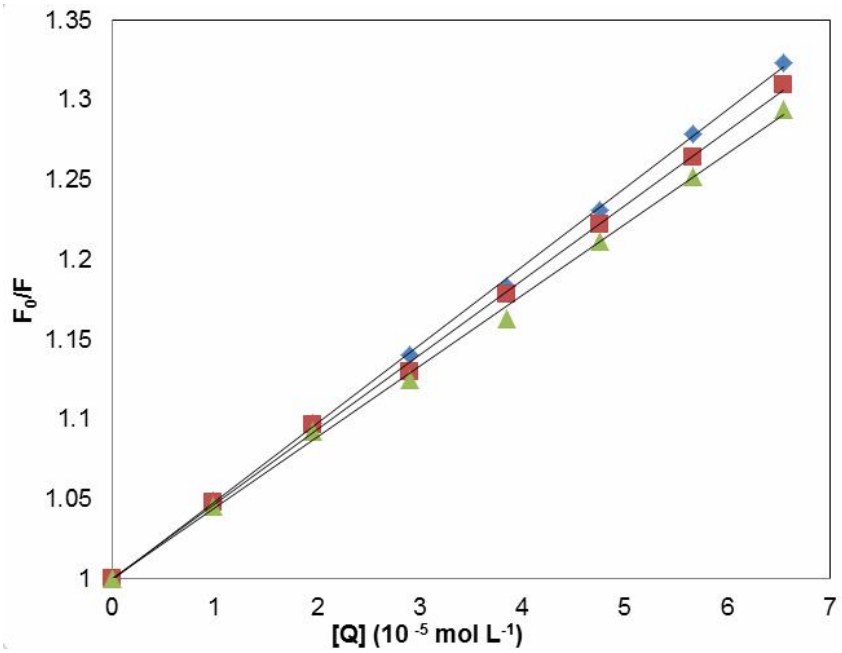

Fig. 3. Stern-Volmer plots for HSA quenching by Etofylline at 298 K (◆), 303 K (■) and 310 K (▲) temperatures.

Table 1. The Stern-Volmer Quenching Constants of HSA-etofylline Interaction

T (K)	$K_{sv} \times 10^3$ (M^{-1})	$K_q \times 10^{11}$ (M^{-1} s^{-1})	R^{2a}
298	4.90 ± 0.05	4.90 ± 0.05	0.9995
303	4.67 ± 0.09	4.67 ± 0.09	0.9990
310	4.43 ± 0.05	4.43 ± 0.05	0.9983

[a]Linear correlated coefficient.

Table 2. The Binding Constants, Number of Binding Sites (n), and Thermodynamic Parameters of HSA-etofylline Interaction

T (K)	$K_a \times 10^3$ (M^{-1})	n	R^{2a}	ΔH (kJ mol^{-1})	ΔG (kJ mol^{-1})	ΔS (J mol^{-1} K^{-1})
298	4.92 ± 0.23	0.988	0.999		-20.95	
303	4.65 ± 0.16	0.971	0.997	-5.71	-21.20	51.14
310	4.31 ± 0.20	0.970	0.997		-21.56	

[a]Linear correlated coefficient.

The K_{sv} values were calculated by the linear regression of Stern-Volmer plots, given in Table 1. Inspecting the results show that K_{sv} values decrease with the rising temperature, which is an indication of static quenching mechanism. Calculated K_q values (reported in Table 1), which are greater than the maximum collision quenching rate constant (2.0×10^{10} M^{-1} s^{-1}), demonstrate that the quenching caused by etofylline is initiated by the formation of complex between etofylline and HSA [44-45].

Binding Parameters

The binding constant (K_a) and the average number of binding sites for one protein molecule (n) of the etofylline-HSA system were determined using the modified Hill equation [11,45,46]:

$$\log \frac{F_0 - F}{F} = n \log K_a + n \log\{[Q_t]\} - \frac{F_0 - F}{F_0}[P_t]\} \qquad (2)$$

where $[Q_t]$ and $[P_t]$ are the total concentrations of ligand and protein, respectively. F_0 and F are the same as the corresponding parameters in Eq. (1).

By linear fitting of Eq. (2), the values of K_a and n at three different temperatures were calculated and summarized in Table 2. Inspecting K_a values reveals their inverse correlation with temperature. This observation is in accordance with the temperature dependence of K_{sv} values and further proof for the static quenching mechanism of HSA by Etofylline [41].

In other words, decrease of K_a values with increasing temperature is due to the destabilization of HSA-etofylline complex [40] confirming the exothermic complex formation between these two compounds [47]. Calculated n values, reported in Table 2, are all close to 1.0, since each HSA molecule has only one binding site for etofylline.

Thermodynamic Parameters and Characteristics of the Binding Forces

The major forces involved in ligand-protein interaction are electrostatic, hydrogen bonding, van der Waals and

hydrophobic interactions. In order to specify the dominant forces in our studied complex, some thermodynamic parameters, able to reveal the interaction nature, were calculated. In this respect, the entropy and enthalpy changes (ΔS and ΔH) were obtained using the Van′t Hoff equation, which relates the binding constant (K) to these two thermodynamic parameters:

$$\ln K = -\frac{\Delta H}{RT} + \frac{\Delta S}{R} \quad (3)$$

Plotting lnK *vs*. 1/T in the above equation, along with determination of the slope and intercept of this linear fitting, gives rise to the ΔH and ΔS values, respectively [46]. Later substitution of these quantities in the following equation results in the Gibbs free energy change at the corresponding temperature:

$$\Delta G = \Delta H - T\Delta S \quad (4)$$

The sign and magnitude of these three thermodynamic parameters were employed to assess the forces involved in the drug-protein complex formation, by Ross and Subramanian [48].

According to the data provided in Table 2, the negative ΔG values (ΔG < 0) at all studied temperatures, demonstrate the spontaneity of HSA-Etofylline complex formation [46,49]. On the other hand, the reaction is exothermic, accompanied by releasing energy. This is realized due to the obtained negative ΔH values (ΔH < 0). The positive values of another thermodynamic property (ΔS > 0) show that the system's entropy increases when HSA-Etofylline complex is formed. This can be attributed to the more disorder in the solution layer adjacent to the protein, after heat releases through the exothermic complex formation.

There are more information hidden in the signs of these three quantities (ΔG, ΔH and ΔS). A positive ΔS value confirms the presence of hydrophobic interaction, while the negative ΔH value is a sign of hydrogen bonding and van der Waals interactions. Hence, the HSA and etofylline entities are kept together by the simultaneous function of hydrophobic, hydrogen bonding and van der Waals interactions [11,40]. Moreover, the docking results (reported in 3.10 section) also confirm this intuition.

Synchronous Fluorescence Spectroscopy

SFS can unravel the conformational alterations of the Tyr and Trp residues by the changes of the maximum emission wavelength (λ_{max}) [21]. In our study, the intensity of SFS decreases with increasing amounts of etofylline, while no shift in the λ_{max} position is recorded (Figs. 4a and b). This observation indicates that binding of etofylline to HSA does not alter the microenvironment around the Tyr and Trp residues.

It should be mentioned that the quenching of SFS is more obvious when Δλ is equal to 60 nm. This points out the more sensitivity of intrinsic fluorescence of Trp, to the HSA-Etofylline interaction, while compared to the intrinsic fluorescence of Tyr [23].

CD Spectra Analysis

The phenomenon of circular dichroism (CD) is very sensitive to the secondary structure of polypeptides and proteins, so CD spectra analysis can be used to study protein conformational and structural alterations, upon interaction with drug. The CD spectra of HSA, both in the absence and presence of etofylline were recorded in order to determine how the etofylline binding, affects the secondary structure of HSA. The CD spectrum of HSA, (Fig. 5) shows two negative peaks at 208 nm (π-π*) and 222 nm (n-π*), characteristic of the α-helix structure of protein. The following two formulas provide more detailed information about the α-helical contents of HSA:

$$MRE = \frac{observed\ CD\ (m\deg)}{10 C_p n l} \quad (5)$$

$$\alpha - Helix\ (\%) = \frac{-MRE_{208} - 400^{\circ}}{3300^{\circ} - 400^{\circ}} \quad (6)$$

where observed CD is the ellipticity in mdeg and MRE_{208} is the result of CD in terms of the mean residue ellipticity in deg cm^2 $dmol^{-1}$ at 208 nm. C_p is the molar concentration of HSA, n, the number of amino acid residues (585), and l, the path length of cell in cm. 4000 is the MRE value of the β-form and random coil conformation and 33000 is MRE of a pure α-helix, both of them at 208 nm [47,50-51].

Adding different amounts of etofylline to the HSA solution eventuated a reduction in the intensity of both

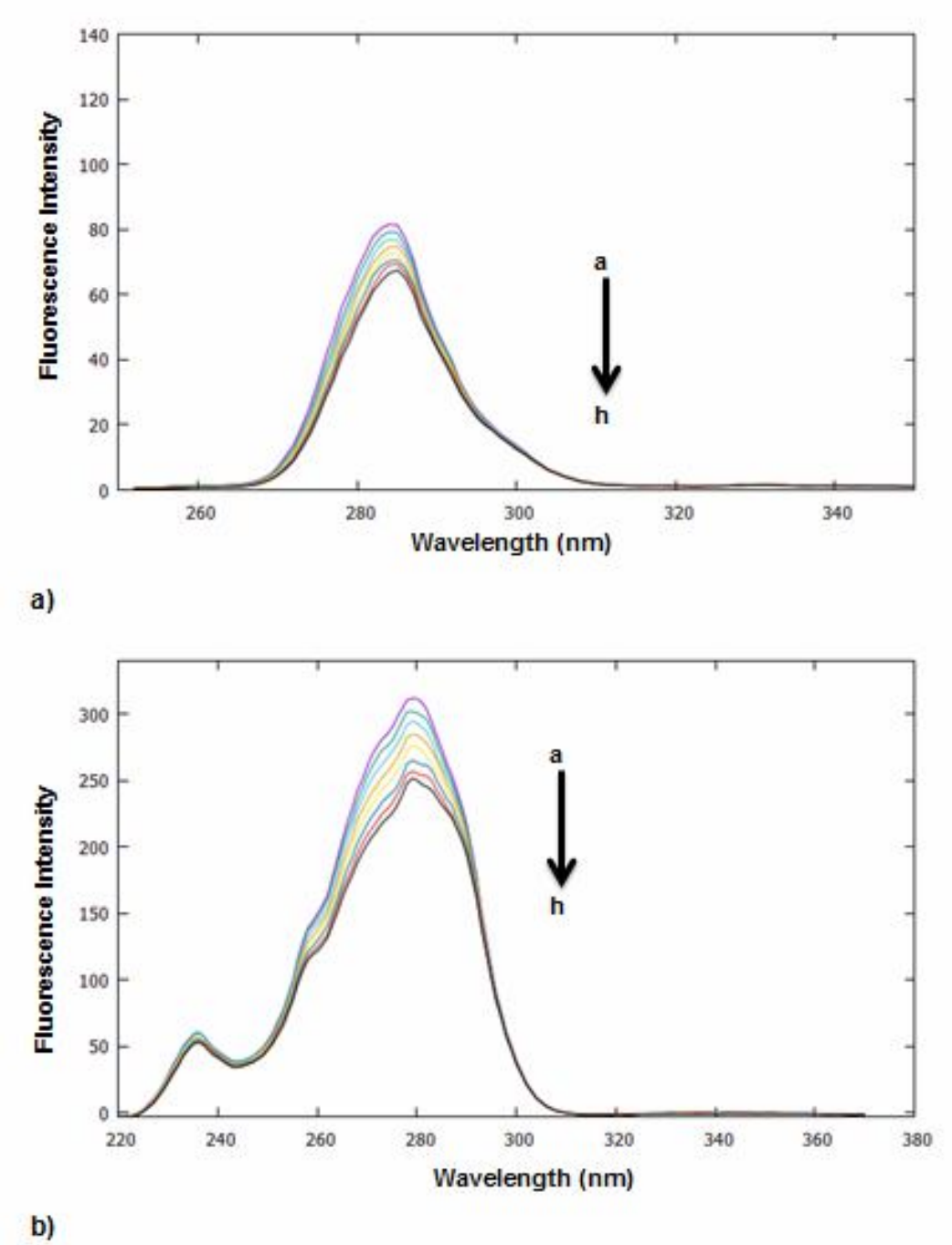

Fig. 4. Synchronous fluorescence spectra for HSA in absence and presence of different amounts of Etofylline stock solution (1 mM) with $\Delta\lambda$ = 15 nm (a) and $\Delta\lambda$ = 60 nm (b), respectively. [(a-h) corresponds to 0, 10, 20, 30, 40, 50, 60 and 70 µl Etofylline].

negative bands of CD spectra, suggesting the change in the protein's secondary structure. No alteration in the shape and peak position of HSA CD spectra (after binding to etofylline), reveals that this protein remains predominantly α-helical, although it loses some helical stabilities. This implies that etofylline molecule binds mainly to the HSA

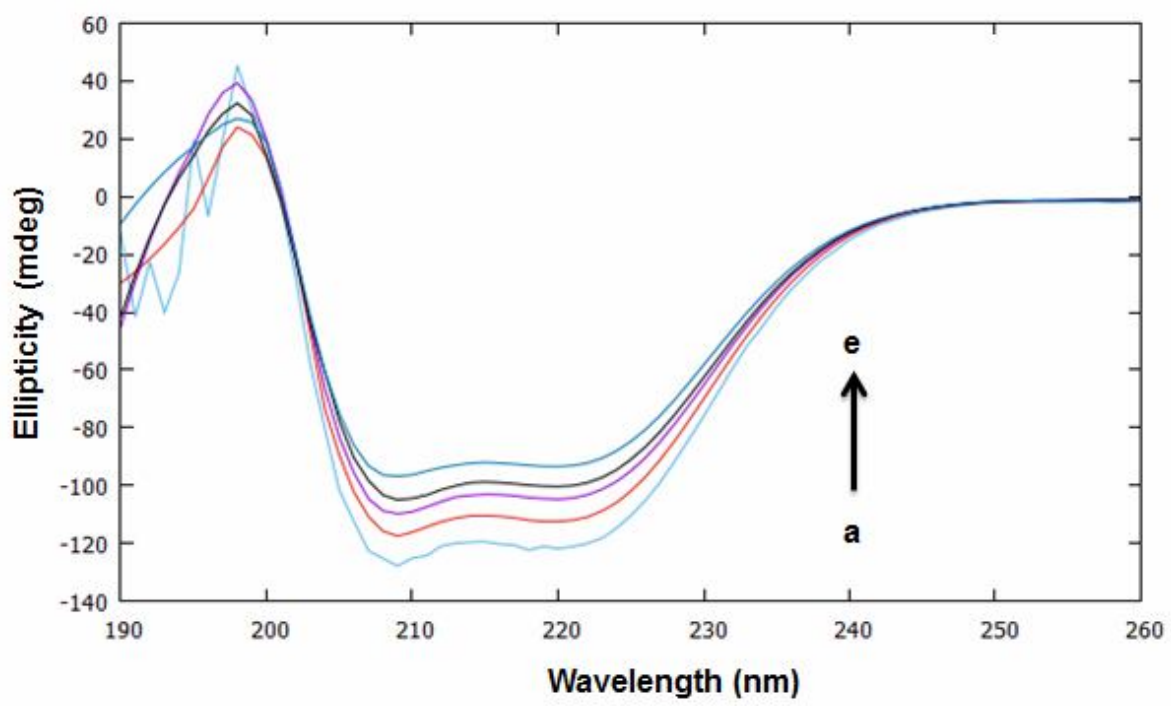

Fig. 5. CD spectra of HSA (10 μM) in absence and presence of Etofylline stock solution (1 mM) at pH 7.4 and room temperature. [(a-e) corresponds to 0, 20, 40, 60 and 80 μl Etofylline].

Table 3. Secondary Structural Features of HSA in the Absence and Presence of 20, 40, 60 and 80 μl Etofylline Stock Solution (1 mM) at pH 7.4 and Room Temperature

Samples	%α-helix	%Antiparallel	%Parallel	%β-turn	%Rndm.Coil
HSA	67.1	2.9	3.1	12.0	13.9
HSA + 20 μl drug	61.8	3.5	3.7	12.7	16.2
HSA + 40 μl drug	57.9	3.9	4.2	13.2	18.0
HSA + 60 μl drug	54.7	4.4	4.6	13.7	19.4
HSA + 80 μl drug	50.9	4.9	4.9	14.2	21.3

surface and does not penetrate inside its structure [52,53].

According to Table 3, showing the results of CD spectroscopic analysis, by addition of different amounts of drug, the α-helical content of HSA decreases, while an increment in β-turn and random coil structures is observable, evidencing the partial protein destabilization

[54,55].

Energy Transfer between Protein and Etofylline

The average distance (r) from the fluorophore (Trp214) to the bound etofylline is easy to obtain using fluorescence resonance energy transfer (FRET) theory. According to the Forster's theory, the energy transfer will occur when the fluorescence emission spectrum of Trp214 (as a donor) and UV-Vis absorption spectrum of etofylline (as an acceptor) have appropriate overlap. We employed this theory to determine the distance between donor and acceptor through the following equations [43,52,56,57]:

$$E = 1 - \frac{F}{F_0} = \frac{R_0^6}{R_0^6 + r^6} \tag{7}$$

$$R_0^6 = 8.8 \times 10^{-25}\ K^2\ N^{-4}\ J \tag{8}$$

$$J = \frac{\int F(\lambda)\varepsilon(\lambda)\lambda^4\, d\lambda}{\int F(\lambda) d(\lambda)} \tag{9}$$

where r is the distance between etofylline and HSA, E, the efficiency of energy transfer, R_0, the critical distance at which the efficiency of energy transfer is 50%, and F and F_0 are the fluorescence intensities of HSA in the presence and absence of etofylline, respectively. k^2 is the spatial orientation factor of the dipole (2/3), n, the refractive index of the medium (1.33), Φ, the fluorescence quantum yield of the donor (0.118), and J, the spectral overlap of the fluorescence emission spectrum of the donor and the absorption spectrum of the acceptor [58]. F (λ) is the fluorescence intensity of the donor and ε (λ), the molar absorption coefficient of etofylline, when the wavelength is λ [44].

Figure 6 shows the spectral overlap of the fluorescence emission of HSA and absorption spectra of etofylline. Calculated parameters from the above equations are $J = 1.72 \times 10^{-15}$ $cm^3\ M^{-1}$, $R_0 = 1.83$ nm and r = 2.17 nm. These results demonstrate the high possibility of energy transfer between HSA and etofylline, because the r value is in the order of 2-8 nm, in agreement with the condition of $0.5R_0 < r < 1.5R_0$ [44,53]. Furthermore, the r value provides an additional evidence for the static quenching mechanism, in accordance to the results of fluorescence quenching [7].

Molecular Dynamics Simulation

The structures of HSA and HSA-etofylline complex were simulated separately in order to obtain their equilibrated structures, under pseudo physiological conditions.

After achieving the equilibrium, the root mean square deviations, radius of gyrations and secondary structures were analyzed for both pure HSA and HSA-etofylline complex. Figure 7 shows the simulation box of HSA-etofylline complex at the end of 20 ns MDS.

Root mean square deviations. Commonly, the convergence of the simulation towards equilibrium is inspected from the relaxation of structure, in terms of the Cartesian distance of final structure from the specified reference one. In this respect, the time revolution of backbone root mean square deviation (RMSD) of HSA in both simulations was analyzed.

As seen in Fig. 8, at 310 K, the backbone RMSD values of free HSA first increased steadily for 15 ns of simulation time, then oscillated around the average value of 0.56 nm, and went to remain almost constant, mainly after 18 ns.

This is an indication of quasi-equilibrium state for HSA. However, more simulation time is needed for HSA to achieve its final equilibrium structure. In the case of HSA-etofylline complex, the backbone RMSD of HSA only increased by 0.2 nm during 20 ns of simulation time. It shows the stability of complex structure and the tight binding of HSA to etofylline in a way that its backbone motion has been restricted.

Radius of gyration. Analysis of the radius of gyration (Eq. (10)) of protein helps to discover its structure's compactness [6],

$$R_g = \left(\frac{\sum_i \|r_i\|^2\, m_i}{\sum_i m_i} \right)^2 \tag{10}$$

where m_i and r_i are the mass and position of atom i with respect to the molecule′s center of mass, respectively.

Figure 9 represents the radius of gyration changing with simulation time for the two simulated systems. In both cases, R_g values reached a plateau at about 15 ns, where free HSA showed slightly higher R_g ones. Binding of etofylline to HSA resulted in decreasing protein's R_g values, which clearly reveals the conformational changes of HSA, upon

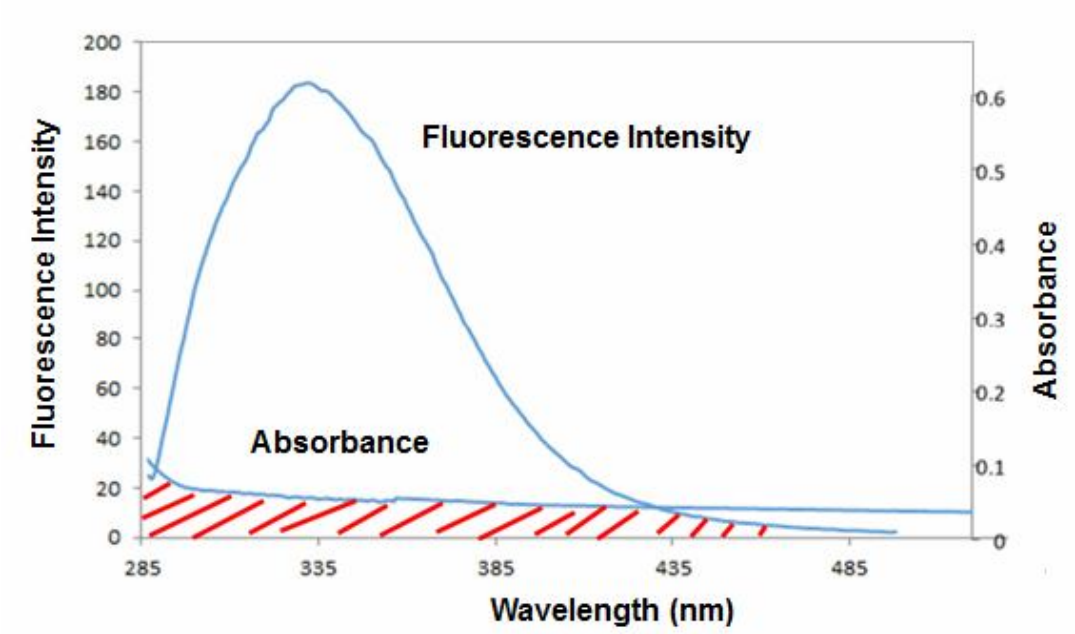

Fig. 6. Overlap of the fluorescence emission of HSA (5μM) and absorption spectrum of Etofylline (5μM), respectively.

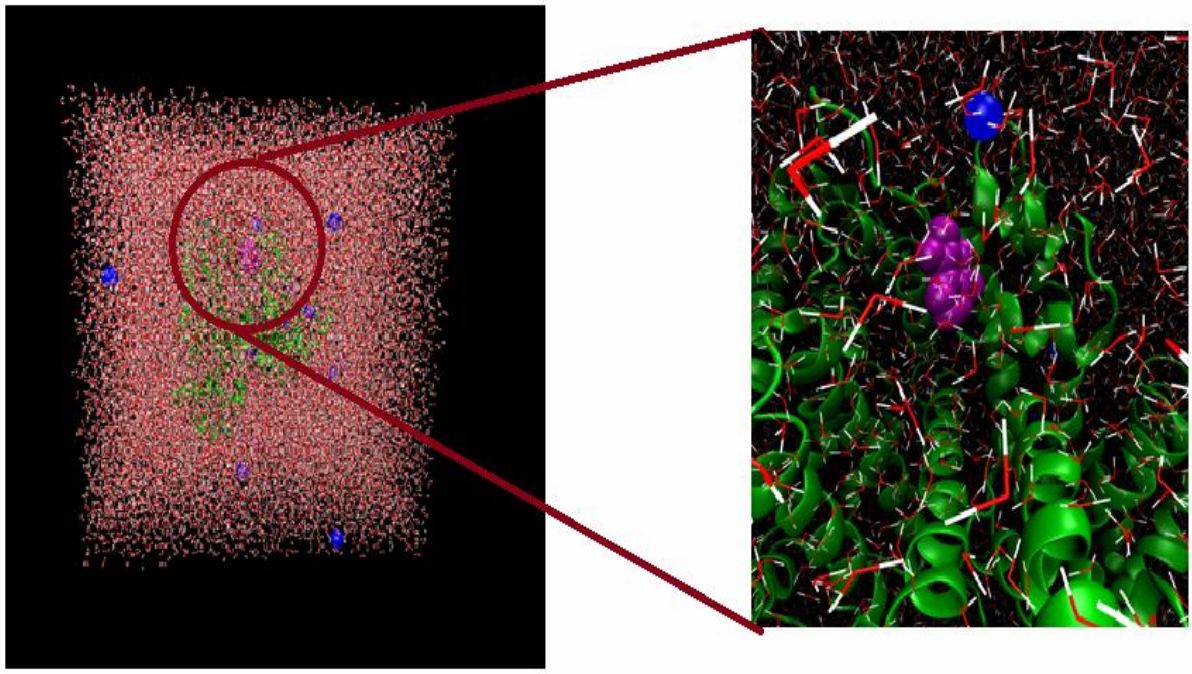

Fig. 7. MD simulation box of HSA-Etofylline complex. The HSA is colored green (newcartoon representation) while Etofylline is shown purple. Water and ions are demonstrated with red&white lines and blue spheres, respectively.

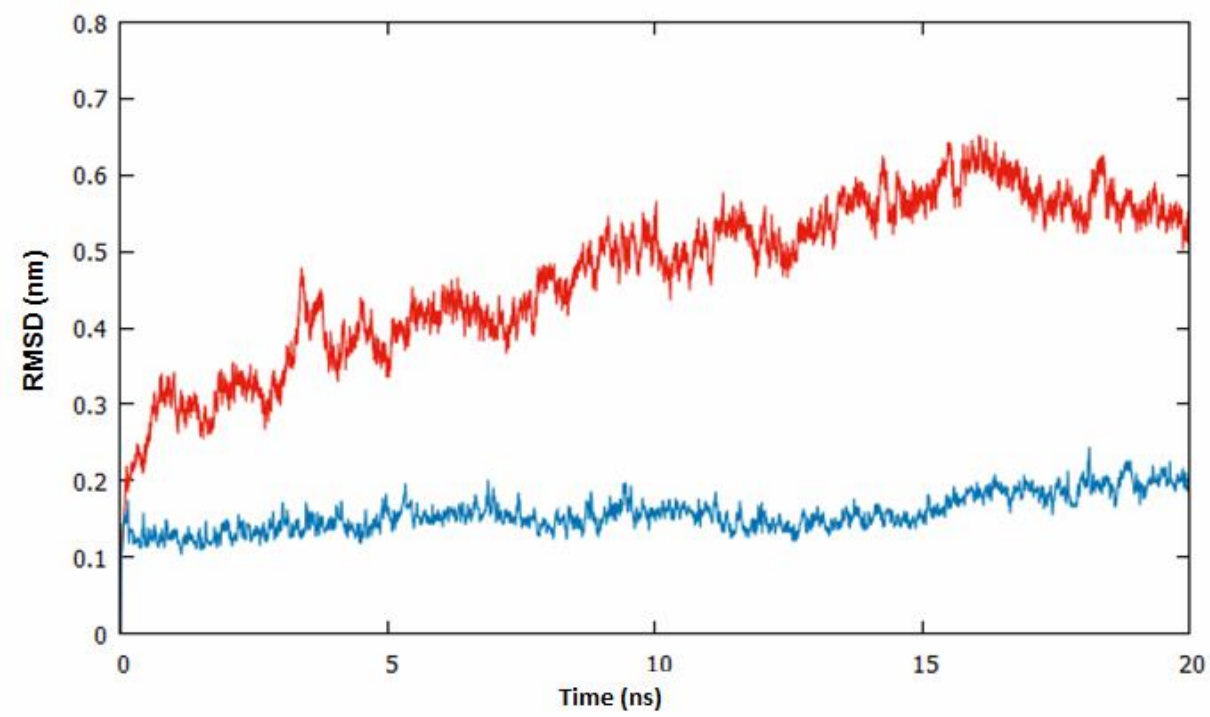

Fig. 8. The backbone root mean square deviation (nm) of free HSA (up) and HSA-Etofylline complex (down).

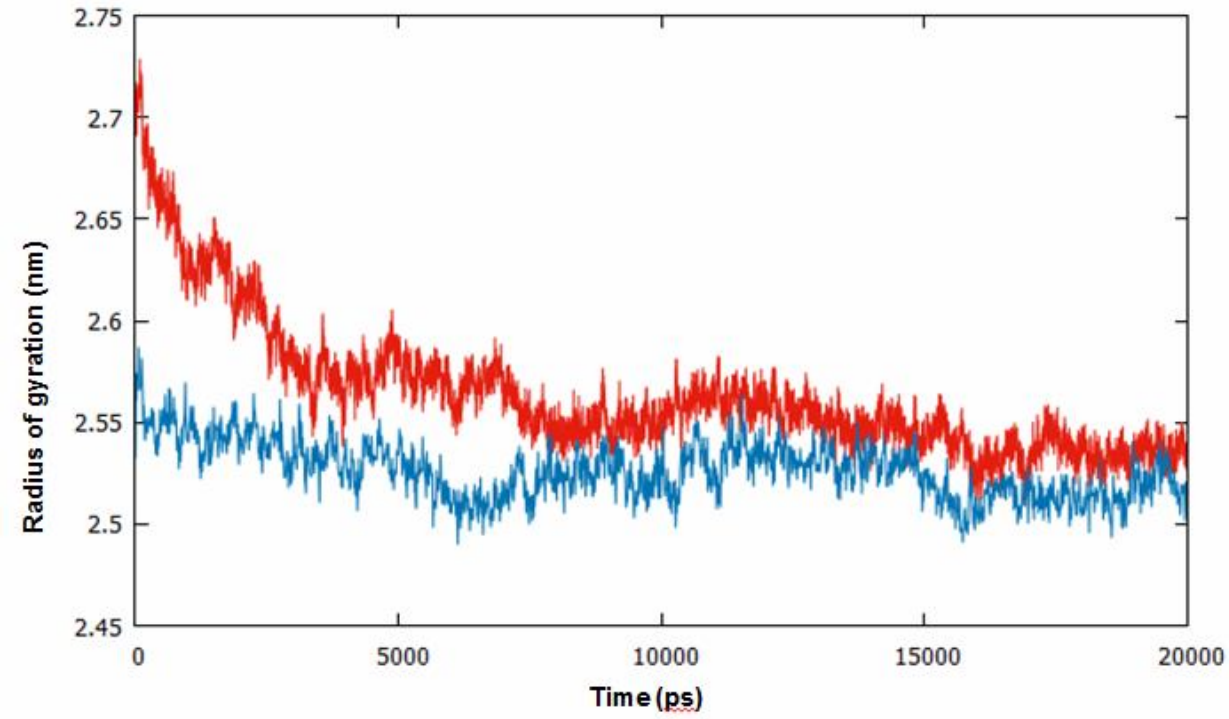

Fig. 9. Time dependence of the radius of gyration (Rg) for the free HSA (up) and HSA-Etofylline complex (down).

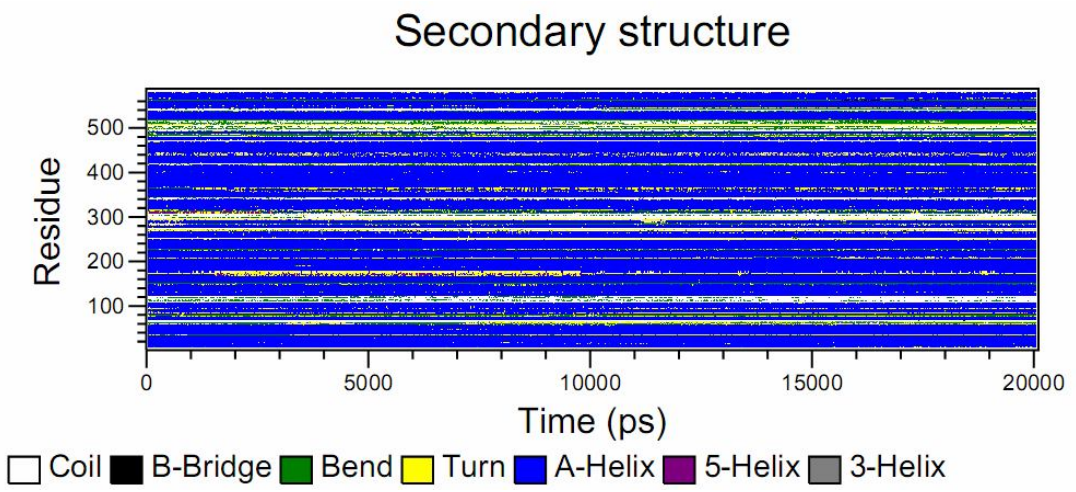

Fig. 10. Variation of the secondary structures *versus* time for HAS-Etofylline system.

Table 4. Structural Features of HSA before and after Molecular Dynamics Simulation (MDS) Taken from the DSSP Method

System	%Coil	%β-Bridge	%Bend	%Turn	%α-Helix	%5-Helix	%3-Helix
HSA	14	0.0	7	7	71	0.0	1
HSA-Etofylline	14	0.0	8	8	69	0.0	0.0

binding to the etofylline structure.

Secondary structure analysis. The secondary structure analysis of the HSA was carried out by do_DSSP command in Gromacs simulation package. Figure 10 and Table 4 show the results of this program [59], providing the information about α-helix and other secondary structural contents of HSA. As shown in Table 4, the α-helix content of HSA in the free and complex forms are 71% and 69%, respectively.

Slightly decreasing the α-helix content of HSA is in agreement with the CD results confirming that etofylline interacts with the HSA residues and reduces the protein's conformational stability. Inspecting the values of different secondary structural parameters of HSA reveals that the protein only changes slightly after being complexed to etofylline. Hence, the interaction of this drug with HSA leads to some microenvironmental changes in the protein's neighborhood.

Molecular Docking Analysis

Molecular docking can provide better understanding of protein-drug interactions. We employed the Auto Dock Vina to predict the complex conformations with the lowest energy, along with the corresponding binding sites. As mentioned in the introduction section, HSA has three homologous domains (I, II and III where each of them consists of two subdomains (A and B)). These three domains include residues (1-195), (196-383) and (384-585), respectively [6,60]. According to Fig. 11, etofylline is surrounded by Gln 104, His 105, Lys106, Val 462, Leu 463, Lys 466 and Thr 467 residues on HAS and is located in

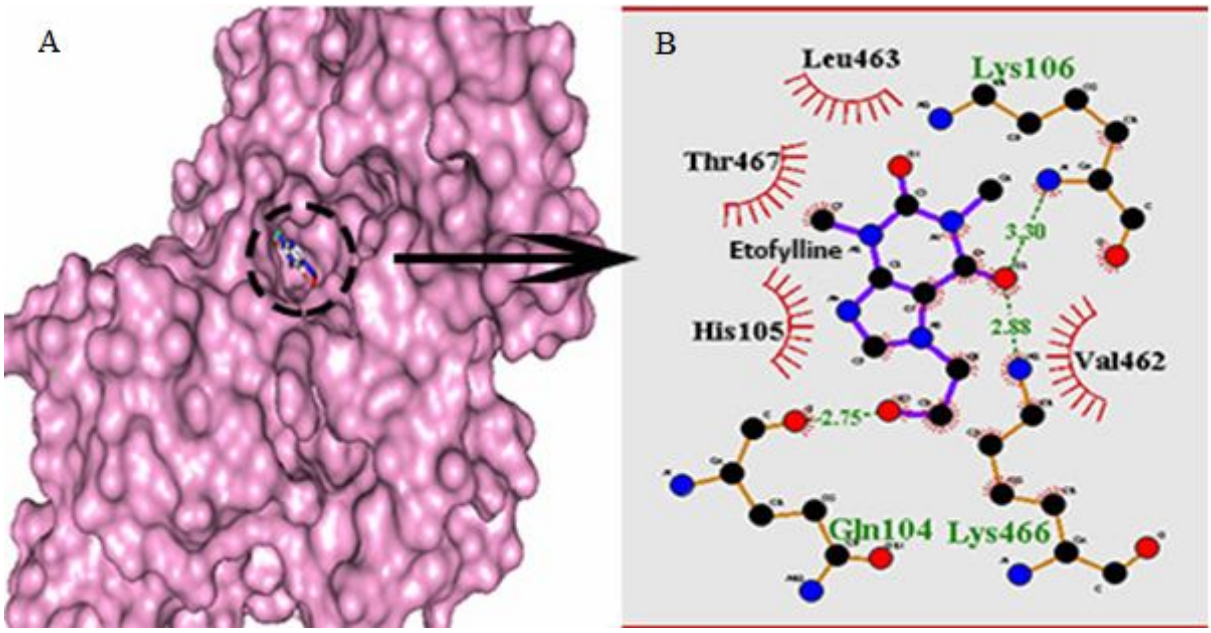

Fig. 11. (A) Molecular surface representation of docked Etofylline in domain I of HSA. (B) LIGPLOT result showing HSA residues, interacting with Etofylline. Hydrogen bonds are indicated by green dashed lines between the atoms involved, while hydrophobic contacts are represented by an arc with spokes radiating towards the ligand atoms they contact. The contacted atoms are shown with spokes radiating back.

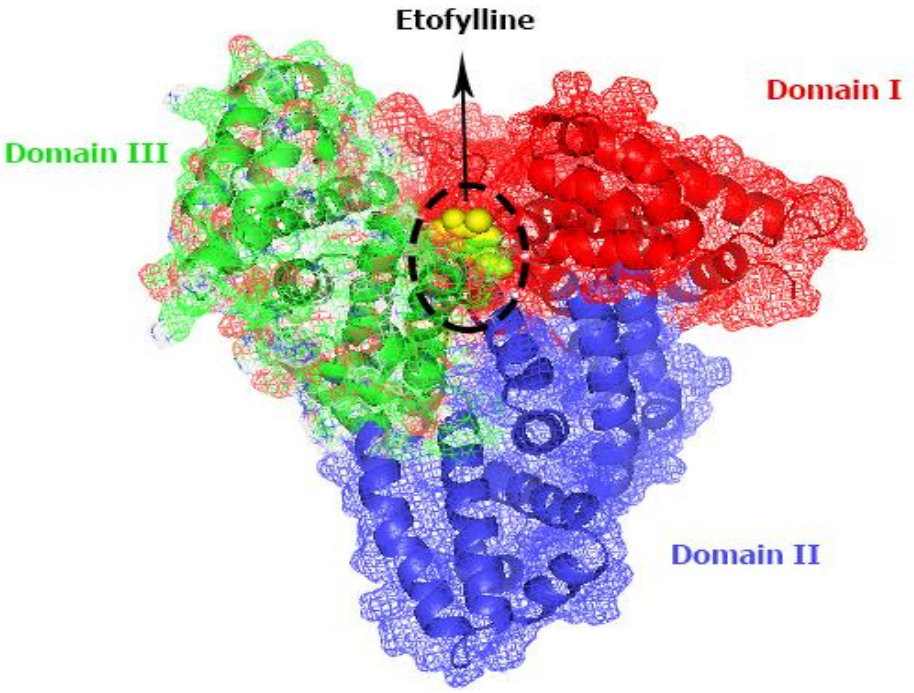

Fig. 12. Etofylline drug docked into domain I of Human Serum Albumin.

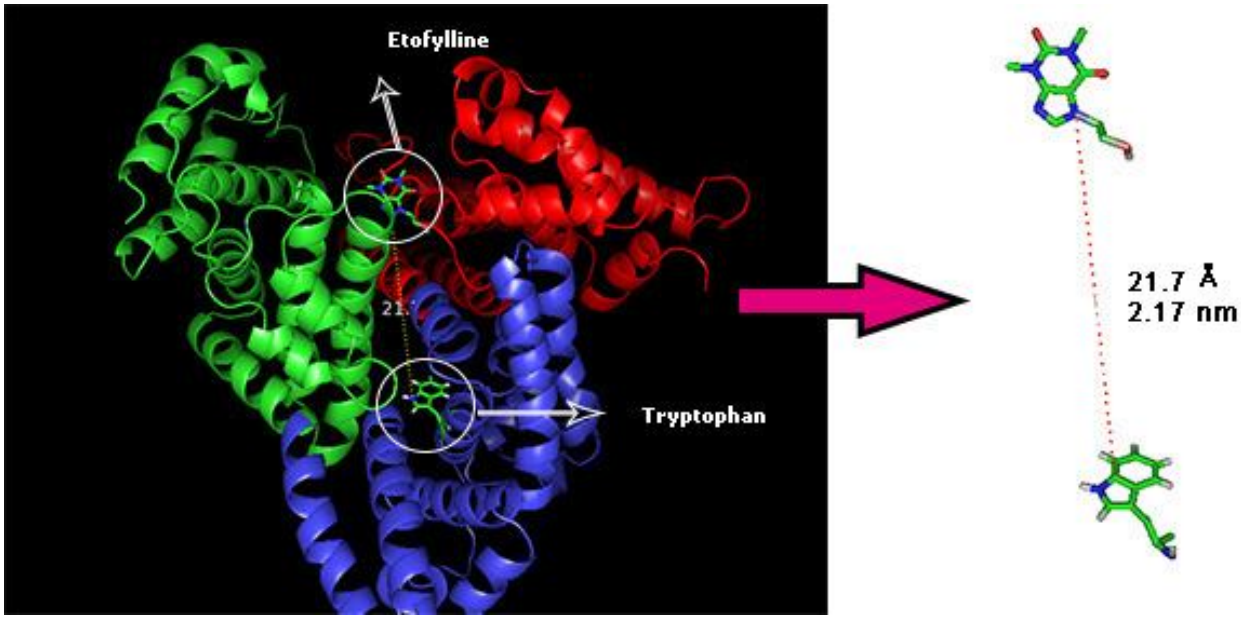

Fig. 13. The distance between Trp-214 of Etofylline in minimum energy docking pose, presented by stick model, using pymol.

domain I of HSA (Fig. 12). Visualization of docking results showed that these residues stabilize etofylline in its binding site by hydrophobic and hydrogen bonding interactions.

The distance between etofylline and Trp-214 was calculated in minimum energy docking pose, shown in Fig. 13. Calculated distance (21.7 Å = 2.17 nm) is in good accordance with the FRET's outcome. (Section 3.8)

CONCLUSIONS

In this study, spectroscopic methods in combination with molecular docking and molecular dynamics simulations were utilized to assess the interaction between the fluorescent protein, HSA with etofylline drug. Obtained results showed that etofylline binds to HSA and quenches its fluorescence through protein-drug complex formation and static quenching mechanism. Moreover the CD and secondary structural analyses of the MDS results exhibited decreasing α-helical content of HSA upon drug addition.

All these observations confirm the conformational changes in the HSA structure. Analysis of thermodynamic parameters using the van′t Hoff equation reveals that hydrophobic and hydrogen bonding interactions are responsible for the stability of etofylline-HSA complex. Molecular docking analysis also shows that etofylline binds to domain I of HSA through hydrophobic and hydrogen bonding interactions. Our overall findings provide better understanding of etofylline-HSA interactions in microscopic details and is beneficial in pharmacy, pharmacology, and biochemistry, as the obtained results help to determine the effective drug dosages.

ACKNOWLEDGEMENTS

The authors would like to thank Shiraz University of Technology for supporting this project.

REFERENCES

[1] Rakotoarivelo, N. V.; Perio, P.; Najahi, E.; Nepveu, F., Interaction between antimalarial 2aryl3hindol-3-one derivatives and human serum albumin. *J. Phys. Chem. B.* **2014**, *118*, 13477-13485, DOI: 10.1021/jp507569e.

[2] Cui, F. -L.; Fan, J.; Lib, J. -P.; Hu, Z. -D., Interactions between 1-benzoyl-4-*p*-chlorophenyl thiosemi-

carbazide and serum albumin: investigation by fluorescence spectroscopy. *Bioorg. Med. Chem.* **2004**, *12*, 151-157, DOI: 10.1016/j.bmc.2003.10.018.

[3] Zhang, X.; Gao, R.; Li, D.; Yin, H.; Zhang, J.; Cao, H.; Zheng, X., Study on interaction between 5-bromo-4-thio-20-deoxyuridine and human serum albumin by spectroscopy and molecular docking. *Spectrochim. Acta, PartA.* **2015**, *136*, 1775-1781, DOI: 10.1016/j.saa.2014.10.081.

[4] He, X. M.; Carter, D. C., Atomic structure and chemistry of human serum albumin. *Nature*, **1992**, *358*, 209-215, DOI: 10. 1038/364362b0.

[5] Yuan, J. -L.; lv, Z.; Liu, Z. -G.; Hu, Z.; Zou, G. -L., Study on interaction between apigenin and human serum albumin by spectroscopy and molecular modeling. *J. Photochem. Photobiol.* **2007**, *191*, 104-113, DOI: 10.1016/j.jphotochem.2007.04.010

[6] Moeinpour, F.; Mohseni-Shahri, F. S.; Malaekeh-Nikouei, B.; Nassirli, H., Investigation into the interaction of losartan with human serum albumin and glycated human serum albumin by spectroscopic and molecular dynamics simulation techniques: A comparison study. *Chem. Biol. Interact.* **2016**, *257*, 4-13, DOI: 10.1016/j.cbi.2016.07.025.

[7] An, X.; Zhao, J.; Cui, F.; Qu, G., The investigation of interaction between thioguanine and human serum albumin by fluorescence and modeling. *Arabian. J. Chem.* **2017**, *10*, S1781-S1787, DOI: 10.1016/j.arabjc.2013.06.031

[8] Shahabadi, N.; Falsafi, M.; Hadidi, S., Molecular modeling and multispectroscopic studies of the interaction of hepatitis B drug, adefovir dipivoxil with human serum albumin. *J. Lumin.* **2015**, *167*, 339-346, DOI: 10.1016/j.jlumin.2015.07.006

[9] Alavianmehr, M. M.; Yousefi, R.; Keshavarz, F.; Mohammad-Aghaie, D., Probing the binding of thioTEPA to human serum albumin using spectroscopic and molecular simulation approaches. *Can. J. Chem.* **2014**, *92*, 1066-1073, DOI: 10.1139/cjc-2013-0571.

[10] Fani, N.; Bordbar, A. K.; Ghayeb, Y., Spectroscopic, docking and molecular dynamics simulation studies on the interaction of two Schiff base complexes with human serum albumin. *J. Lumin.* **2013**, *141*, 166-172, DOI: 10.1016/j.jlumin.2013.03.001.

[11] Zahirul Kabir, M.; Mukarram, A. K.; Mohamad, S. B.; Alias, Z.; Tayyab, S., Characterization of the binding of an anticancer drug, lapatinib to human serum albumin. *J. Photochem. Photobiol., B.* **2016**, *160*, 229-239. DOI: 10.1016/j.jphotobiol.2016.04.005.

[12] Bai, H. -X.; Liu, X. -H.; Yang, F.; Yang, X. -R., Interactions of human serum albumin with phenothiazine drugs: Insights from fluorescence spectroscopic studies. *J. Chin. Chem. Soc.* **2009**, *56*, 696-702, DOI:10.1002/jccs.200900104.

[13] Peng, X.; Wang, X.; Qi, W.; Su, R.; He, Z., Affinity of rosmarinic acid to human serum albumin and its effect on protein conformation stability. *Food Chem.* **2016**, *192*, 178. DOI: 10.1016/j.foodchem.2015.06.109.

[14] Abdollahpour, N.; Soheili, V.; Saberi, M. R.; Chamani, J., Investigation of the interaction between human serum albumin and two drugs as binary and ternary systems. *Eur. J. Drug Metab. Pharmacokinet.* **2016**, 41, 705-721, DOI: 10.1007/s13318-015-0297-y.

[15] Islam, M. M.; Sonu, V. K.; Gashnga, P. M.; Moyon, N. S.; Mitra, S., Caffeine and sulfadiazine interact differently with human serum albumin: A combined fluorescence and molecular docking study. *Spectrochim. Acta, Part A.* **2016**, *152*, 23-33, DOI: 10.1016/j.saa.2015.07.051.

[16] Nirav, P. M.; Kaushal, K. C., validation and stability study for simultaneous estimation of etofylline and theophylline by RP-HPLC chromatography in marketed formulation. *J. Chem. Pharm. Res.* **2011**, *3*, 597-609, DOI:10.4172/2155-9872.1000116.

[17] Tripathi, K. D., Essentials of Medical pharmacology, 7th Ed., New Dehli, India, 2013.

[18] Kleemann, A.; Engel, J.; Kutscher, B.; Reichert, D., Pharmaceutical Substances, 5th Ed, Thieme, Stuttgart, 2008.

[19] Ranjbar, S.; Shokoohinia, Y.; Ghobadi, S.; Bijari, N.; Gholamzadeh, S.; Moradi, N.; Ashrafi-Kooshk, M. R.; Aghaei, A.; Khodarahmi, R., Studies of the interaction between isoimperatorin and human serum albumin by multi spectroscopic method: Identification of possible binding site of the compound using esterase activity of the protein. *Sci. World J.* **2013**, *2013*, 1-13, DOI: 10.1155/2013/305081.

[20] Li, Y. -Q.; Li, X. -Y.; Falih Shindi, A. A.; Zou, Z. -X.; Liu, Q.; Lin, L. -R.; Li, N., Synchronous fluorescence spectroscopy and Its applications in clinical analysis and food fafety evaluation, part of the reviews in fluorescence book series, *RFLU*, **2010**, 95-117. DOI: 10.1007/978-1-4419-9828-6_5.

[21] Sudha, A.; Srinivasan, P.; Thamilarasan, V.; Sengottuvelan, N., Exploring the binding mechanism of 5-hydroxy-3,4,7-trimethoxyflavone with bovine serum albumin: Spectroscopic and computational approach. *Spectrochim. Acta, Part A.* **2016**, *157*, 170-181, DOI: 10.1016/j.saa.2015.12.028.

[22] Xi, L.; Wang, Y.; He, Q.; Zhang, Q.; Du, L., Interaction between Pin1 and its natural product inhibitor epigallocatechin-3-gallate by spectroscopy and molecular dynamics simulations. *Spectrochim. Acta, Part A.* **2016**, *169*, 134-143, DOI: 10.1016/j.saa.2016.06.036.

[23] Samari, F.; Shamsipur, M.; Hemmateenejad, B.; Khayamian, T.; Gharaghani, S., Investigation of the interaction between amodiaquine and human serum albumin by fluorescence spectroscopy and molecular modeling. *Eur. J. Med. Chem.* **2012**, *54*, 255-263, DOI: 10.1016/j.ejmech.2012.05.007.

[24] Miller, J. N., Recent advances in molecular luminescence analysis, *Proc. Anal. Div. Chem. Soc.* **1979**.

[25] Van der Spoel, D.; Lindahl, E.; Hess, B.; Groenhof, G.; Mark, A. E.; Berendsen, H. J. C., GROMACS: fast, flexible, and free. *J. Comput. Chem.* **2005**, *26*, 1701-1718, DOI:10.1002/jcc.20291

[26] van Gunsteren, W. F.; Billeter, S. R.; Eising, A. A.; Hüenberger, P. H.; Krüger, P.; Mark, A. E.; Scott, W.; Tironi, W. R. P., Biomolecular Simulation: The GROMOS 96 Manual and User Guide; Swiss Federal Institute of Technology: Zurich, Switzerland, 1996.

[27] Kennard, E. H., Kinetic Theory of Gases; McGraw-Hill: New York, 1963.

[28] Berendsen, H. J. C.; Postma, J. P. M.; Van Gunstetren, W. F.; Hermans, J., Interaction Models for Water in Relation to Protein Hydration. In Intermolecular Forces. Pullman, B., Ed.; Reidel: Dordrecht, The Netherlands, 1981, pp. 331-342.

[29] Hirshman, S. P.; Whitson, J. C., Steepest-descent moment method for three-dimensional magnetohydrodynamic equilibria. *Phys. Fluids* **1983**, *26*, 3553-3568, DOI: 10.1063/1. 864116.

[30] Parrinello, M.; Rahman, A., Polymorphic transitions in single crystals: A new molecular dynamics method. *J. Appl. Phys.* **1981**, *52*, 7182-7190, DOI: 10.1063/1.328693.

[31] Berendsen, H. J. C.; Postma, J. P. M.; Van Gunsteren, W. F.; DiNola, A.; Haak, J. R., Molecular dynamics with coupling to an external bath. *J. Chem. Phys.* **1984**, *81*, 3684-3690, DOI: 10.1063/1.448118.

[32] Darden, T.; York, D.; Pedersen, L., Particle mesh Ewald: An N-log(N) method for Ewald sums in large systems. *J. Chem. Phys.* **1993**, *98*, 10089-10092, DOI: 10.1063/1.464397.

[33] Essmann, U.; Perera, L.; Berkowitz, M. L.; Darden, T.; Lee, H.; Pedersen, L. G., A smooth particle mesh Ewald method. *J. Chem. Phys.* 1995, *103*, 8577-8582, DOI: 10.1063/1.470117.

[34] Berendsen, H.; Postma, J. P. M.; Van Gunsteren, W. F.; Hermans, J., in: B. Pullman (Ed.), Intermolecular Forces, D Reidel Publishing Company, Dordrecht, The Netherlands, 1981.

[35] Miyamoto, S.; Kollman, P. A., SETTLE: An analytical version of the shake and rattle algorithm for rigid water models. *J. Comput. Chem.* **1992**, *13*, 952-962, DOI: 10.1002/jcc.540130805.

[36] Schuttelkopf, A. W.; van Aalten, D. M. F., PRODRG: a tool for high-throughput crystallography of protein-ligand complexes. *Acta Crystallogr. Sect. D: Biol. Crystallogr.* **2004**, *60*, 1355-1363, DOI: 10.1107/S0907444904011679.

[37] Frisch, M. J.; Trucks, G. W.; Schlegel, H. B.; Scuseria, G. E.; Robb, M. A.; Cheeseman, J. R., *et al.* Gaussian, Inc., Wallingford CT, 2009.

[38] Trott, O.; Olson, A. J., AutoDock Vina: improving the speed and accuracy of docking with a new scoring function, efficient optimization, and multithreading. *J. Comput. Chem.* **2010**, *31*, 455-461, DOI: 10.1002/jcc.21334.

[39] Streitwieser, A., Molecular Orbital Theory for Organic Chemists, Wiley: New York, 1961.

[40] Tayyab, S.; Izzudin, M. M.; Zahirul Kabir, M.; Feroz, S. R.; Tee, W. -V.; Mohamad, S. B.; Alias, Z.,

Binding of an anticancer drug, axitinib to human serum albumin: Fluorescence quenching and molecular docking study. *J. Photochem. Photobiol.* **2016**, *162*, 386-394, DOI: 10.1016/j.jphotobiol.2016.06.049.

[41] Abdelhameed, A. S.; Alanazi, A. M.; Bakheit, A. H.; Darwish, H. W.; Ghabbour, H. A.; Darwish, I. A., Fluorescence spectroscopic and molecular docking studies of the binding interaction between the new anaplastic lymphoma kinase inhibitor crizotinib and bovine serum albumin. *Spectrochim. Acta, Part A.* **2017**, *171*, 174-182, DOI: 10.1016/j.saa.2016.08.005.

[42] Ajmal, M. R.; Nusrat, S.; Alam, P.; Zaidi, N.; Vahid Khan, M.; Zaman, M.; Shahein, Y. E.; Mahmoud, M. H.; Badr, G.; Hasan Khan, R., Interaction of anticancer drug clofarabine with human serum albumin and human -1 acid glycoprotein. Spectroscopic and molecular docking approach. *J. Pharm. Biomed. Anal.* **2017**, *135*, 106-115, DOI: 10.1016/j.jpba.2016.12.001.

[43] Lakowicz, J. R., Principles of Fluorescence Spectroscopy, 2nd Ed, New York, 1999.

[44] Daneshgar, P.; Moosavi-Movahedi, A. A.; Norouzi, P.; Ganjali, M. R., Molecular interaction of human serum albumin with paracetamol: Spectroscopic and molecular modeling studies. *Int. J. Biol. Macromol.* **2009**, *45*, 129-134, DOI: 10.1016/j.ijbiomac.2009.04.011

[45] Lu, D.; Zhao, X.; Zhao, Y.; Zhang, B.; Zhang, B.; Geng, M.; Liu, R., Binding of Sudan II and Sudan IV to bovine serum albumin: Comparison studies. *Food Chem. Toxicol.* **2011**, *49*, 3158-3164, DOI: 10.1016/j.fct.2011.09.011.

[46] Shahraki, S.; Shiri, F.; Saeidifar, M., Evaluation of in silico ADMET analysis and human serum albumin interactions of a new lanthanum(III) complex by spectroscopic and molecular modeling studies. *Inorg. Chim. Acta*. **2017**, *463*, 80-87, DOI: 10.1016/j.ica.2017.04.023.

[47] Yuan, L.; Liu, M.; Liu,G.; Li, D.; Wang, Z.; Wang, B.; Han, J.; Zhang, M., Competitive binding of (-)-epigallocatechin-3-gallate and 5-fluorouracil to human serum albumin: A fluorescence and circular dichroism study. *Spectrochim. Acta, Part A*. **2017**, *173*, 584-592, DOI: 10.1016/j.saa.2016.10.023.

[48] Ross, P. D.; Subramanian, S., Thermodynamics of protein association reactions: Forces contributing to stability. *Biochemistry,* **1981**, *20*, 3096. DOI: 10.1021/bi00514a017.

[49] Kabir, M. Z.; Tee, W. -V.; Mohamad, S. B.; Alias, Z.; Tayyab, S., Comprehensive insight into the binding of sunitinib, a multi-targeted anticancer drug to human serum albumin. *Spectrochim. Acta, Part A.* **2017**, *181*, 254-263, DOI: 10.1016/j.saa.2017.03.059.

[50] Ma, X.; Yan, J.; Xu, K.; Guo, L.; Li, H., Binding mechanism of trans-N caffeoyltyramine and human serum albumin: Investigation by multi-spectroscopy and docking simulation. *Bioorg. Med. Chem.* **2016**, *66*, 102-110, DOI: 10.1016/j.bioorg.2016.04.002.

[51] Wang, Q.; Sun, Q.; Ma, X.; Rao, Z.; Li, H., Probing the binding interaction of human serum albumin with three bioactive constituents of Eriobotrta japonica leaves: Spectroscopic and molecular modeling approaches. *J. Photochem. Photobiol.* **2015**, *148*, 268-276, DOI: 10.1016/j.jphotobiol.2015.04.030.

[52] Abdullah, S. M. S.; Fatma, S.; Rabbani, G.; Ashraf, J. M., A spectroscopic and molecular docking approach on the binding of tinzaparin sodium with human serum albumin. *J. Mol. Struct.* **2017**, *1127*, 283-288, DOI: 10.1016/j.molstruc.2016.07.108.

[53] Wang, J.; Ma, L.; Zhang, Y.; Jiang, T., Investigation of the interaction of deltamethrin (DM) with human serum albumin by multi-spectroscopic method. *J. Mol. Struct.* **2017**, *1129*, 160-168, DOI: 10.1016/j.molstruc.2016.09.061

[54] Laurini, E.; Marson, D.; Posocco, P.; Fermeglia, M.; Pricl, S., Structure and binding thermodynamics of viologen-phosphorous dendrimers to human serum albumin: a combined computational/experimental investigation. *Fluid Phase Equilib.,* **2016**, *422*, 18-31, DOI: 10.1016/j.fluid.2016.02.014.

[55] Ariga, G. G.; Naik, P. N.; Chimatadar, S. A.; Nandibewoor, S. T., Interactions between epinastine and human serum albumin: Investigation by fluorescence, UV-Vis, FT-IR, CD, lifetime measurement and molecular docking. *J. Mol. Struct.* **2017**, *1137*, 485-494, DOI: 10.1016/j.molstruc.2016.12.066.

[56] Fani, N.; Bordbar, A. K.; Ghayeb, Y., A combined spectroscopic, docking and molecular dynamics

simulation approach to probing binding of a Schiff base complex to human serum albumin. *Spectrochim. Acta, Part A.* **2013**, *103*, 11-17, DOI: 10.1016/j.saa.2012.11.003.

[57] Byadagi, K.; Meti, M.; Nandibewoor, S.; Chimatadar, S., Investigation of binding behaviour of procainamide hydrochloride with human serum albumin using synchronous, 3D fluorescence and circular dichroism, *J. Pharm. Anal.* **2017**, *7*, 103-109, DOI: 10.1016/j.jpha.2016.07.004.

[58] Rub, M. A.; Masood Khan, J.; Azum, N.; Asiri, A. M., Influence of antidepressant clomipramine hydrochloride drug on human serum albumin: Spectroscopic study. *J. Mol. Liq.* **2017**, *241*, 91-98, DOI: 10.1016/j.molliq.2017.05.143.

[59] Kabsch, W.; Sander, C., Dictionary of protein secondary structure: pattern recognition of hydrogen-bonded and geometrical features. *Biopolymers,* **1983**, *22*, 2577-2637, DOI: 10.1002/bip.360221211.

[60] Wang, Q.; Sun, Q.; Ma, X.; Rao, Z.; Li, H., Probing the binding interaction of human serum albumin with three bioactive constituents of Eriobotrta japonica leaves: Spectroscopic and molecular modeling approaches. *J. Photochem. Photobiol. B: Biol.* **2015**, *148*, 268-276, DOI: 10.1016/j.jphotobiol.2015.04.030.